Journal of Cerebral Blood Flow & Metabolism (2009), 1–12
© 2009 ISCBFM All rights reserved 0271-678X/09 $32.00
www.jcbfm.com

On the fate of extracellular hemoglobin and heme in brain

Flavio A Lara[1,2,3], Suzana A Kahn[1], Anna CC da Fonseca[1], Carlomagno P Bahia[4], João PC Pinho[4], Aurélio V Graca-Souza[2], Jean C Houzel[4], Pedro L de Oliveira[2], Vivaldo Moura-Neto[1] and Marcus F Oliveira[5,6]

[1]*Laboratório de Morfogênese Celular, Departamento de Anatomia, Instituto de Ciências Biomédicas, Universidade Federal do Rio de Janeiro, Cidade Universitária, Rio de Janeiro, Brazil;* [2]*Programa de Biologia Molecular e Biotecnologia, Laboratório de Bioquímica de Artrópodes Hematófagos, Instituto de Bioquímica Médica, Universidade Federal do Rio de Janeiro, Cidade Universitária, Rio de Janeiro, Brazil;* [3]*Laboratório de Microbiologia Celular, Instituto Oswaldo Cruz, Rio de Janeiro, Brazil;* [4]*Laboratório de Fronteiras em Neurociências, Programa de Neurociências Básico e Clínico, Instituto de Ciências Biomédicas, UFRJ;* [5]*Programa de Biologia Molecular e Biotecnologia, Laboratório de Bioquímica Redox, Instituto de Bioquímica Médica, Universidade Federal do Rio de Janeiro, Cidade Universitária, Rio de Janeiro, Brazil;* [6]*Laboratório Associado de Inflamação e Metabolismo, Instituto Nacional de Biologia Estrutural e Bioimagem, Universidade Federal do Rio de Janeiro, Cidade Universitária, Rio de Janeiro, Brazil*

Intracerebral hemorrhage (ICH) is a major cause of disability in adults worldwide. The pathophysiology of this syndrome is complex, involving both inflammatory and redox components triggered by the extravasation of blood into the cerebral parenchyma. Hemoglobin, heme, and iron released therein seem be important in the brain damage observed in ICH. However, there is a lack of information concerning hemoglobin traffic and metabolism in brain cells. Here, we investigated the fate of hemoglobin and heme in cultured neurons and astrocytes, as well as in the cortex of adult rats. Hemoglobin was made traceable by conjugation to Alexa 488, whereas a fluorescent heme analogue (tin-protoporphyrin IX) was prepared to allow heme tracking. Using fluorescence microscopy we observed that neurons were more efficient in uptake hemoglobin and heme than astrocytes. Exposure of cortical neurons to hemoglobin or heme resulted in an oxidative stress condition. Viability assays showed that neurons were more susceptible to both hemoglobin and heme toxicity than astrocytes. Together, these results show that neurons, rather than astrocytes, preferentially take up hemoglobin-derived products, indicating that these cells are actively involved in the ICH-associated brain damage.
Journal of Cerebral Blood Flow & Metabolism advance online publication, 1 April 2009; doi:10.1038/jcbfm.2009.34

Keywords: intracerebral hemorrhage; orphyrin; reactive oxygen species; toxicity; trauma

Introduction

Cerebrovascular diseases and their consequences, including strokes, represent the second most frequent cause of death, after ischemic heart diseases. Intracerebral hemorrhage (ICH) has been estimated to account for 10% to 15% (Sudlow and Warlow, 1997) of the 5.7 million deaths caused annually by stroke worldwide (WHO, 2006). More importantly, ICH has an unfavorable prognosis, with an extremely high mortality rate in the first month (approximately 45%) and the majority of survivors show debilitating neurologic sequels (Fogelholm *et al*, 1992). The pathophysiology of ICH comprises a complex chain of events starting with blood–brain barrier disruption and infiltration of blood components into the brain parenchyma, resulting in a progressive edema, which starts in the first 24 h and remains elevated during several days (Koeppen *et al*, 2004). In many cases, inflammatory cell recruitment and activation contribute to the cerebral parenchyma damage, resulting

Correspondence: Dr FA Lara, Laboratório de Microbiologia Celular, Sala 27, Pavilhão Hanseníase, Fundação Oswaldo Cruz, Instituto Oswaldo Cruz, Av Brasil, número 4365, CEP 21045-900, Rio de Janeiro, Brazil.
E-mail: falara@ioc.fiocruz.br
This study was supported by CNPq (through Institutos Nacionais de Ciência e Tecnologia 2008), FAPERJ (MFO through Jovens Cientistas do Nosso Estado 2007 and Edital de Apoio a Grupos Emergentes de Pesquisa do Rio de Janeiro, 2008), ICGEB, HHMI.
Received 26 August 2008; revised 10 March 2009; accepted 13 March 2009

in neuronal death, not only inside, but also around the perifocal reactive zone (Gong *et al*, 2000; Rogers *et al*, 2003).

The destructive action of blood components to the central nervous system can be analyzed under two overlapping perspectives: inflammation and oxidative stress. Heme has recently been shown to be an immunoactive molecule, able to promote neutrophil and macrophage activation and migration both *in vitro* and *in vivo* (Figueiredo *et al*, 2007; Porto *et al*, 2007; Graça-Souza *et al*, 2002). The free-radical hypothesis for ICH is based on the cytotoxicity triggered by blood components and its degradation products, such as heme and iron. Heme catabolism by heme oxygenase (HO) results in the release of carbon monoxide, biliverdin, and iron. Although HO is frequently described as an antioxidant enzyme, it is well known that iron is a potent pro-oxidant atom, capable to generate highly reactive oxygen species, such as hydroxyl, alkoxyl, and peroxyl radicals (Ryter and Tyrrell, 2000). Curiously, derrangements in iron metabolism have been described in other neuropathologies, such as Alzheimer's neurodegenerative disorder (Smith *et al*, 1997).

Although much progress has been made toward the functions of HO activity and iron metabolism in the brain, the cellular mechanisms involved in the clearance of blood components during an ICH episode are still not well understood. There is a consensus that a first wave of microglial recruitment occurs in areas surrounding the lesion 24 to 48 h after the hemorrhage, followed by recruitment of blood phagocytes that are essential to blood clot resolution and, later, by the invasion of neutrophils (Gong *et al*, 2000). However, intracortical injections of purified hemoglobin seem to interfere dramatically with brain physiology, as this promotes epileptic seizures (Rosen and Frumin, 1979). In agreement with this finding, reductions in plasma levels of haptoglobin are also associated with epileptic seizures (Panter *et al*, 1985).

A number of observations converge to the fact that hemoglobin toxicity is cell specific, being neurons more sensitive than astrocytes (Rogers *et al*, 2003; Chen-Roetling and Regan, 2006; Regan and Panter, 1993). Conversely, HO-1 is involved in astrocyte and neuron heme tolerance (Regan *et al*, 2000; Chen-Roetling and Regan, 2006), whereas the function of HO-2 in neuronal protection against heme remains controversial (Doré *et al*, 1999; Rogers *et al*, 2003). Zinc protoporphyrin IX, a potent HO inhibitor, has recently shown to be beneficial in a rabbit model of ICH, indicating that iron released from heme degradation may be involved in the pathogenesis of ICH (Gong *et al*, 2006). Expression of HO-1 and ferritin during ICH suggested that not only microglia, but also astrocytes, were involved in hemoglobin digestion, heme degradation, and subsequent iron storage (Koeppen *et al*, 1995; Turner *et al*, 1998). These findings strongly suggest that hemoglobin, heme, and iron are pivotal in the pathogenesis of ICH-induced brain damage.

To understand the fate of hemoglobin and heme in the brain after ICH, we monitored the localization of these molecules in neurons and astrocytes both *in vitro* and *in vivo*, using a fluorescent heme analogue and/or fluorescent-labeled hemoglobin. We show that neurons were more efficient in the uptake of globin, hemoglobin, and a heme analogue, compared with astrocytes. In addition, neurons revealed to be more susceptible to hemoglobin and heme than astrocytes, in a mechanism involving oxidative stress.

Materials and methods

Primary Astrocyte and Neuronal Cell Cultures

Primary cultures of astrocytes were prepared from newborn (0- to 1-day-old) Wistar rat cerebral cortex, as previously described by Gomes *et al*, 1999. Briefly, dissociated cells were plated in Dulbecco's modified Eagle's medium/F12 with 10% fetal bovine serum and expanded in 25 cm^2 tissue culture flasks at 37°C in a humidified 5% CO_2 atmosphere. After 3 days, weakly bound cells, mostly neurons, were washed away. After 1 week, when confluence was achieved, the culture was treated with trypsin and transferred to 15.5 mm diameter poly-L-lysine-treated glass coverslips in 24-well plates for microscopy, or to 96-well plates for viability assays.

Primary neuronal cultures were prepared from embryonic day 18 or newborn (0- to 1-day-old) Wistar rats cerebral cortex, as previously described. Briefly, the cerebral cortices were dissociated in Dulbecco's modified Eagle's medium/F12 medium supplemented with 33 mmol/L glucose, 2 mmol/L glutamine, and 3 mmol/L sodium bicarbonate. From this suspension, 5×10^4 cells were plated on poly-L-lysine-treated coverslips placed on a 24-well plate for neuronal cultures or plated over normal astrocytes monolayers for neuroastrocytes coculture experiments. Both cultures and cocultures were maintained in Dulbecco's modified Eagle's medium/F12 medium without serum to 24 or 48 h. Finally, using cytochemistry staining by isolectin B4 (Sigma, St Louis, MO, USA) we observed that microglia contaminants in our neuronal cultures were approximately 0.5% (data not shown).

Tin-Protoporphyrin IX Fluorescence Analysis

Tin-Protoporphyrin IX (SnPPIX; Frontier Scientific, Logan, UT, USA) solutions were prepared in dimethyl sulfoxide to a final concentration of 20 mmol/L. Then a 10 mmol/L SnPPIX was prepared by diluting this stock solution 1:2 in 0.1 N NaOH. For spectrofluorometric analysis 10 μmol/L SnPPIX solutions were prepared from the 10 mmol/L solution by diluting them in methanol, albumin, or water and data were acquired in a Cary Eclipse spectrofluorimeter (Varian, Palo Alto, CA, USA). To assess SnPPIX uptake, cells were incubated with a 10 μmol/L SnPP IX solution diluted in culture medium without serum for 2 h. Afterwards, cells were washed with phosphate-buffered saline (PBS), fixed in 4% paraformaldehyde, and observed

in an Axioplan 2 epifluorescence microscope (Zeiss, Göttingen, Germany). The fluorescence images were obtained using a filtered 100 W mercury lamp as the excitation light source with a filter set BP 400 to 410 nm/FT 510 nm/LP 515 nm. Quantification of fluorescent intensities was performed by measuring bitmaps generated by ImageJ software (available at http://rsb.info.nih.gov/ij/).

Hemoglobin Labeling

Adult rat hemoglobin was purified as follows: heparinized blood was centrifuged at 100*g* for 10 min and erythrocytes were resuspended in 50 mmol/L Tris-HCl (pH 8.5), with 1.7% NaCl and 1 mmol/L EDTA. This step was repeated twice. After, erythrocytes were lysed in the same buffer without NaCl and cell debris was pelleted by centrifuging at 1,000*g* for 30 mins. Hemoglobin was finally precipitated by salting out in ammonium chloride at 80% saturation for 12 h at 4°C. The insoluble hemoglobin was pelleted by centrifuging at 1,000*g* for 30 min and then solubilized by dialysis against 10 mmol/L phosphate buffer. The final hemoglobin preparation was quantified in five replicates by using the Folin method (Lowry *et al*, 1951). Alexa 488 (Molecular Probes, Eugene, OR, USA) labeling was performed as indicated by the manufacturer. Briefly, 10 μg of Alexa 488 solubilized in dimethyl sulfoxide was added to 10 μg of hemoglobin in 0.1 mol/L sodium bicarbonate buffer (pH 8.3), for 1 h at room temperature. The reaction was stopped by adding 1.5 mol/L hydroxylamine (pH 8.3). Unbound probe was excluded by gel filtration, using PBS as mobile phase. Contamination of endotoxins in all globin, hemoglobin, and heme preparations was assessed by using the Limulus amebocyte lysate assay (QCL-1000; BioWhittaker, Walkersville, MD, USA) following the manufacturer's procedures.

Globin Preparation

The globin solution was prepared as follows: purified hemoglobin from rat blood was denatured and heme was removed in diethylketone (HCl 0.02 mol/L kept in an ethanol) dry ice bath, as described (Teale, 1959). Precipitated protein was washed once and renaturated by sequential dialysis against water.

Stereotaxic Injection of Alexa 488-Hemoglobin in Adult Rat Cerebral Cortex

Wistar male rats ($n = 4$, 3-month old) were obtained from the animal facility at the Universidade Federal do Rio de Janeiro. Experimental procedures followed local rules for use of laboratory animals, based on the *Guide for the Care and Use of Laboratory Animals* (NIH, no. 86-23, revised 1985) and all measures were taken to reduce the number of animals and avoid their suffering. On the following day, anesthesia was induced with an intramuscular mixture of xylazine (4 mg/kg; Rompun, Bayer, Germany) and ketamine chloride (46 mg/kg, Ketalar; Parke-Davis, Detroit, MI, USA). Body temperature was maintained at 37°C through a heating pad, respiration and heart rates were monitored and nociceptive reflexes were checked periodically so that additional doses of anesthetic could be subsequently administered if necessary. After head immobilization in the stereotaxic apparatus, an incision was made through the scalp and the skull overlying the parietal cortex of both hemispheres was opened with a dental drill. At standard stereotaxic coordinates (2.8 mm posterior to bregma and 5.2 mm lateral from the midline) a small incision was opened in the dura and a glass capillary with 40 to 50 μm internal tip diameter, connected through a mineral oil-filled tubing to a Hamilton microsyringe, was lowered 1.200 μm below the pial surface. Four microliters of solutions containing 10 μg of Alexa 488-hemoglobin or 10 μg of unlabeled hemoglobin was slowly injected into the right and left hemispheres, respectively. The opening was closed with Gelfoam and bone wax and the incision was sutured. Animals were allowed to recover with food and water *ad libitum*. After 2 days, they were administered a lethal dose of anesthetic and perfused transcardially with pH 7.4, 0.1 mol/L PBS followed by 4% paraformaldehyde in 0.1 mol/L PBS. The brain was dissected, cryoprotected in 30% buffered sucrose for 12 h, blocked in OCT-TissueTek (Sakura, São Paulo, Brazil), and frozen in liquid nitrogen. Serial, coronal, 15 μm thick sections were cut using a CM1900 cryostat (Leica Microsystems GmbH, Wetzlar, Germany).

Immunolocalization of β-Tubulin III and Glial Fibrillary Acidic Protein

For coronal brain sections, immunohistochemistry for β-tubulin III was performed as follows: sections were blocked using 5% bovine serum albumin and 0.05% Triton X-100 in PBS for 4 h, before overnight incubation at 4°C with mouse anti-β-tubulin III IgG (Promega, Madison, WI, USA) diluted 1:500 in PBS with 1% bovine serum albumin and 0.05% Triton X-100). Sections were then washed and the stained with CY3-conjugated antimouse secondary antibody (Sigma), diluted 1:5,000 in PBS with 1% bovine serum albumin. For culture assays, immunocytochemistry was performed as follows: cultured cells plated on glass coverslips were fixed with 4% paraformaldehyde for 15 mins and permeabilized with 0.2% Triton X-100 in PBS for 5 mins at room temperature. After blocking with 5% bovine serum albumin for 30 mins, cells were incubated with primary antibodies: mouse anti-β-tubulin III IgG (1:1,000) or anti-GFAP IgG (1:500) (Dako, Glostrup, Denmark) overnight at 4°C followed by PBS washes and incubation with antimouse IgG conjugated with CY3 or antirabbit conjugated with fluorescein isothiocyanate (FITC) for 1 h at room temperature, to localize β-tubulin III and glial fibrillary acidic protein (GFAP), respectively. For all immunostainings, negative control sections or plates were performed by omitting the primary antibody. Differential interference contrast images of cultures were obtained using an Axioplan 2 epifluorescence microscope (Zeiss). Epifluorescence images of Alexa 488 and FITC were obtained using a 100 W mercury lamp as the excitation light source with a filter set BP 450 to

490 nm/FT 510 nm/LP 515 nm. 4,6-Diamidino-2-phenyl indole (DAPI) fluorescence was acquired using G 365 nm/FT 395 nm/LP 420 nm filter set, CY3 signal was obtained using BP 545-555 nm/FT 580 nm/LP 590 nm as filter set and BP 410 nm/FT 510 nm/LP 520 nm to observe SnPPIX fluorescence. Confocal images were acquired using a Meta 510 laser scanning microscope (Zeiss), with an excitation laser of 405 nm.

Cellular Viability

Viabilities of cell cultures were assessed by using the MTT (3-[4,5-dimethylthiazol-2-yl]-2,5-diphenyltetrazolium bromide) reduction to formazan assay. Briefly, cells were adhered to 96-well plates and exposed to different conditions in quintuplicate for 12 h. Viability was assessed by adding MTT to the cultures at a final concentration of 500 μmol/L. After 2 h, the supernatant was discarded, cells were disrupted, and formazan was solubilized by addition of lysis buffer as follows: 20% SDS, 50% dimethylformamide, 2% acetic acid, and 2.5% HCl 1 mol/L. Formazan light absorption at 540 nm was determined using a microplate reader Versa Max (Molecular Devices, Sunnyvale, CA, USA). Viability analysis in cocultures was assessed after 12 h of different insults in two independent experiments using four cell cultures for each condition. Dead cells were removed by washing cultures with PBS three times for 5 mins and the number of live cells was determined by counting the number of cells attached to the coverslips. Afterwards, the cells were fixed with 4% paraformaldehyde and finally stained with DAPI 20 μg/mL for 15 mins. Cells were observed in an Axiobserver fluorescence microscope (Zeiss). Differential interference contrast images were used to distinguish neurons from astrocytes in cocultures. In addition, neurons and astrocytes can also be distinguished through the pattern of DAPI staining, as neurons exhibit not only stronger fluorescence signal, compared with astrocytes, but also smaller nucleus.

Statistical Analyses

Comparisons between groups were done by the one-way analysis of variance and *a posteriori* Tukey's test for pairwise comparisons. Differences of $P<0.05$ were considered to be significant. Analysis of variance and Tukey's test were performed by GraphPad Prism version 4.00 for Windows (GraphPad Software, San Diego, CA, USA).

Results

Neurons Uptake SnPPIX more Efficiently than Astrocytes

Our group has recently showed that palladium mesoporphyrin IX is a fluorescent heme analogue that can be used to follow heme traffic in living cells (Lara *et al*, 2005). Previous works have shown that SnPPIX also has potential as a tool for real-time heme-tracking studies (Simionatto *et al*, 1984). In Figure 1A we observe that SnPPIX fluorescence

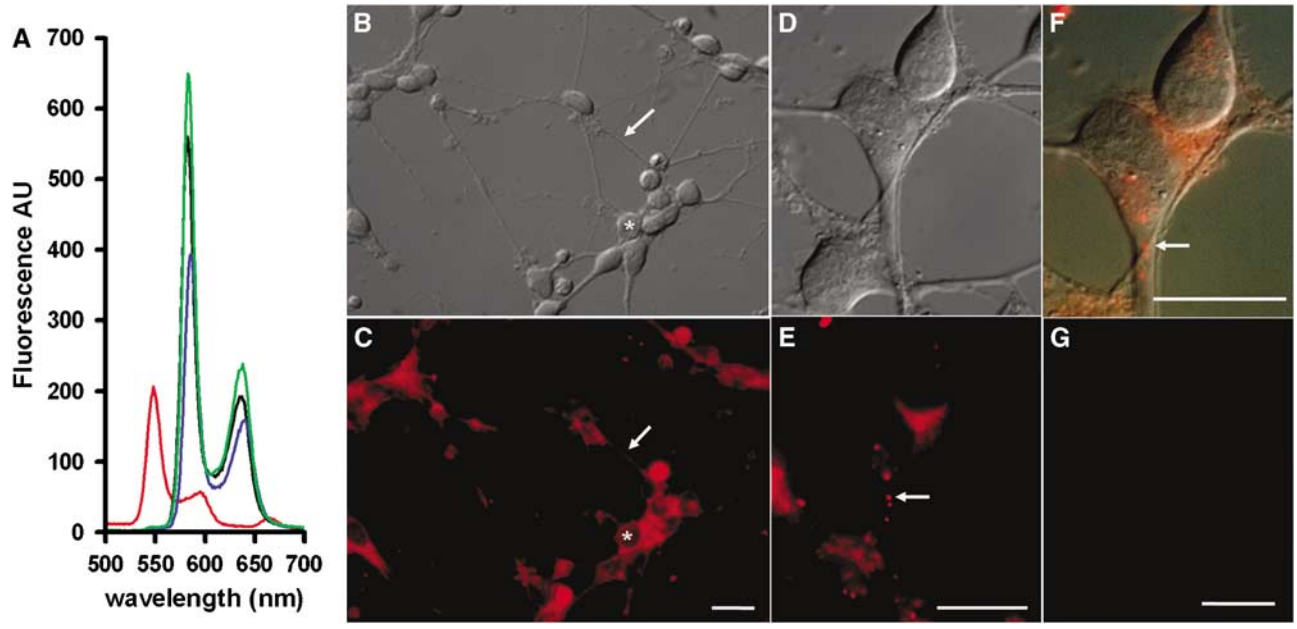

Figure 1 Cortical neurons are able to take up the fluorescent heme analogue tin-protoporphyrin IX (SnPPIX) *in vitro*. (**A**) Spectra of palladium mesoporphyrin IX (red line) and SnPPIX were recorded in water (black line), methanol (green line) or bound to 5 μmol/L albumin (blue line). Spectra were acquired by excitation at 400 nm as described in the Materials and methods section. Neurons derived from 18-day embryonic rat cerebral cortexes were cultured for 24 h and exposed to 10 μmol/L of SnPPIX for 2 h in serum-free medium. Interference contrast (**B** and **D**) or fluorescence images (**C**, **E**, and **G**) were acquired and a merged image (**F**) was constructed. (**C**) Neuronal culture presenting a strong red emission conferred by the porphyrin accumulation along cellular bodies (asterisk) and neurites (arrow). (**E**) Higher magnification images showing the SnPPIX signal located inside small vesicles (arrow), located in a neurite as can be seen in the merged image (**F**). (**G**) Neuronal culture exposed to SnPPIX at 4°C. Scale bar = 20 μm.

emission spectrum is insensitive to changes in the environmental dielectric constant, because it shows the same emission spectra regardless the medium composition. However, SnPPIX exhibited a much higher quantum yield when compared with palladium mesoporphyrin IX, because a 0.5 μmol/L solution presents three times more signal at its maximal emission peak than palladium mesoporphyrin IX 50 μmol/L solution. Taking advantage of these features and also of higher quantum yield of SnPPIX, we were able to follow its uptake and traffic as a heme analogue in rat brain and central nervous system cells.

To compare the uptake of this heme analogue by neurons and astrocytes, we established cell cultures containing almost exclusively neurons, confirmed after 2 days in culture by positive immunocytochemistry against β-tubulin III antigens, and presence of few cells (less than 5%) immunolabeled with GFAP. Then, we exposed neurons from embryonic rat cerebral cortex to 100 μmol/L SnPPIX for 2 h (Figure 1B). The cultured neurons were able to take up considerable amounts of this probe as shown by the accumulation of fluorescence signals in the cell bodies (asterisk in Figure 1C) as well as in the neurites (arrow in Figure 1C). Porphyrins are amphipathic molecules and part of their cytotoxicity is based on their ability to associate with lipid bilayers, disrupting their permeability, and resulting in porphyrin internalization and accumulation (Schmitt *et al*, 1993). To check whether the observed uptake was indeed a passive accumulation of the SnPPIX in the neuronal membranes, higher magnification images were acquired. As shown in Figure 1, the SnPPIX fluorescence was present in the cell body as well as within endocytic vesicles (arrows), showing that a simple, passive partition across neuronal membranes is not the major uptake mechanism for the porphyrin molecules. SnPPIX uptake at 4°C was undetectable on all five experiments performed (Figure 1F). In contrast, GFAP-positive astrocytes from glia-enriched cultures did not display detectable levels of SnPPIX accumulation (Figure 2). Although astrocytes were less efficient in take up SnPPIX, it is possible that the staining can be ascribed to contaminant microglial cells present in our culture conditions (Figure 2C and 2D , asterisks). In these experiments, cultures were exposed to SnPPIX for 2 h in a serum-free medium, to avoid the conjugation of SnPPIX to serum proteins such as albumin. Additional experiments performed in serum-supplemented medium produced similar results, reinforcing the observations that astrocytes were much less prone to take up free, as well as albumin-complexed SnPPIX (data not shown).

More Efficient Hemoglobin Uptake in Neurons Triggers Oxidative Stress

It is well known that in the first days after a brain hemorrhagic event, microglial cells are recruited to the hemorrhagic spot to perform endocytosis and lysosomal digestion of blood constituents (Koeppen *et al*, 1995). Thus, we next investigated whether neurons or astrocytes would be able to take up hemoglobin in a similar manner, by exposing these cells to fluorescent-labeled hemoglobin. The concentrations used were chosen based on those where their cytotoxic effects would be expected to be minimal (Regan and Panter, 1993). Neuron–astrocyte cocultures were prepared and exposed to hemoglobin conjugated to Alexa 488 for 12 h. Figure 3 shows the aspect of the coculture, which appears as a carpet of astrocytes under a layer of neurons. The small round nuclei of neurons were positive for DAPI staining and contrast with the large nuclei of the astrocytes (Figure 3B, asterisks). The neuronal cells were identified in cocultures through specific immunolocalization of β-tubulin III antigens (Figure 3C). Merged images of β-tubulin III and Alexa 488-hemoglobin stainings reveal that the uptake of hemoglobin was much more efficient in neurons than in astrocytes *in vitro* (Figure 3D). Control experiments performed at 4°C showed no detectable amounts of hemoglobin uptake (data not shown).

Hemoglobin is known to be deleterious to the central nervous system, with both neuroexcitatory and neurotoxic effects (Rosen and Frumin, 1979; Sadrzadeh *et al*, 1987). One obvious mechanism for hemoglobin neurotoxicity is through reactive oxygen species formation (Sadrzadeh and Eaton, 1988), which is related to free heme release from hemoglobin digestion and subsequently of free iron from the breakdown of heme by HO-2 in neurons and/or HO-1 in neuronal and glial cells. To assess whether hemoglobin uptake and globin exposure result in oxidative stress conditions in neuronal cytosol, we exposed newborn rat cortical neurons to 10 μmol/L hemoglobin for 4 h and assessed the levels of reactive species by using the fluorescent probe CMH_2-DCFDA (Figure 4). We observed that hemoglobin exposure for 4 h is enough to promote a dramatic redox imbalance and an oxidative stress condition throughout neuronal cell body and neurites (Figure 4A and 4D). Similar to hemoglobin, exposure to heme (Figure 4B and 4E) was able to increase neuronal oxidative stress. Interestingly, oxidative stress mediated by hemoglobin and heme seems not to be a general process because albumin was not able to generate a similar response (Figure 4C). In addition, this phenomenon is not related to an indiscriminate injury compared with the exposure to 1 μmol/L staurosporine (Figure 4F).

Hemoglobin Uptake and Subcellular Distribution is Regionally Distinct in the Brain and Involves Neurons in the Process

Rat brains were exposed to autologous hemoglobin *in vivo*, by injecting hemoglobin-Alexa 488 into

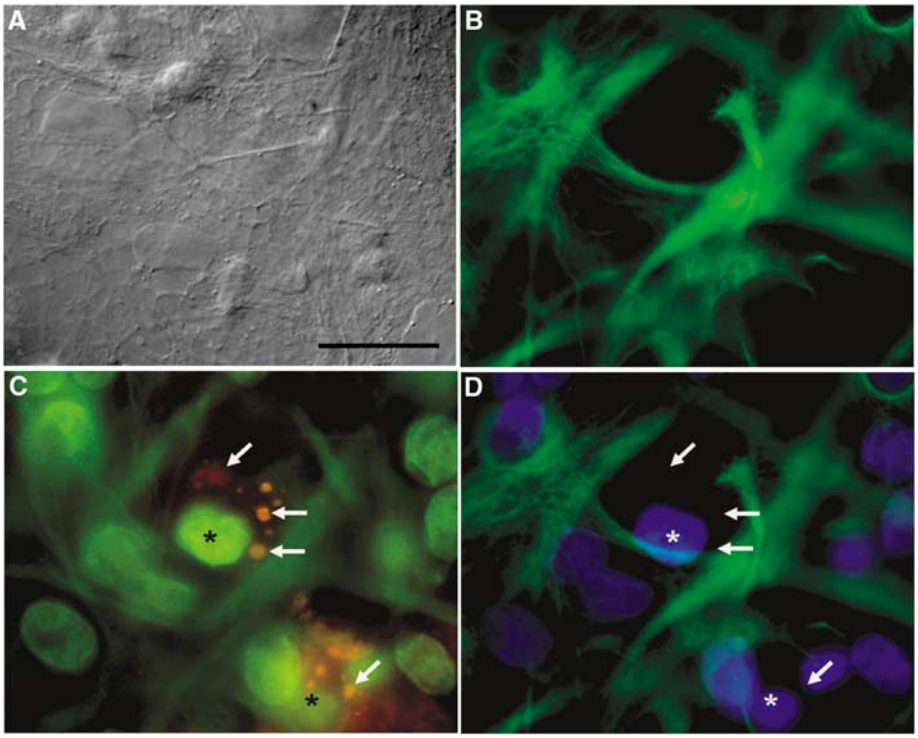

Figure 2 Cortical astrocytes do not uptake the fluorescent heme analogue SnPPIX *in vitro*. Astrocyte-enriched cultures derived from newborn rat cerebral cortex dissociation were cultivated for 24 h and incubated with 10 μmol/L SnPPIX for 2 h deprived of serum. (**A**) Interference image, (**B**) FITC fluorescence image, (**C**) SnPPIX fluorescence image, presenting DAPI and FITC fluorescence leak, and (**D**) DAPI fluorescence image merged with image (**B**). (**A**) Astrocytes-enriched culture presenting heterogeneous aspect; (**B**) GFAP immunocytochemistry showing the position of astrocytes in the field; (**C**) SnPPIX fluorescence in red (arrows) located in nonastrocytic cells (asterisk), DAPI and FITC emission leak is observed in green; (**D**) DAPI emission (blue) appearing in astrocytes and nonastrocyte nuclei (asterisk) merged with GFAP astrocyte images in green (**B**). Scale bar = 20 μm.

the parietal cortex. In all four injected animals, we observed an intense hemoglobin uptake in the parietal cortex and hippocampus, particularly in the CA1 region, which displayed the most intense fluorescence signal (Figure 5A–5F, arrows). A strong hemoglobin uptake was also observed in perivascular regions, probably associated to endothelial cells (Figure 5A–5B, arrowheads). Interestingly, the distribution of hemoglobin-rich endocytic vesicles was different according to the brain region, being rather diffuse in cortical cells and more punctuated in hippocampal cells (Figure 5G–5H). To investigate which cortical cell types were responsible for hemoglobin uptake *in vivo*, β-tubulin III-immunolabeled sections were analyzed by confocal microscopy. Figure 5I shows that β-tubulin III staining surrounds discrete green dots suggesting the presence of hemoglobin-Alexa 488 stain inside endocytic vesicles (arrows).

Hemoglobin Neurotoxic Effects are Mediated by Heme

Because neurons, instead of astrocytes, were more efficient in the uptake of blood products, we assessed the viability of both cell types on the exposure of different compounds (Figure 6). MTT reduction assays showed that hemoglobin, heme, and reconstituted hemoglobin (globin + heme) all exhibited cytotoxic effects on neuronal cultures, compared with control and globin (Figure 6A). All hemoglobin by-products failed to exert a significant deleterious effect on astrocytes cultures (Figure 6B), corroborating previous data from Regan and Panter (1993). In addition, these effects were not related to the presence of microbial-derived contaminants in hemoglobin preparations because the experiments were conducted in the presence of polymyxin B (5 μg/mL; data not shown). Also, addition of *Escherichia coli* lipopolysaccharide (50 ng/mL) caused any neuronal death, as expected by the lower microglia contaminant in these cultures (data not shown).

Finally, we performed experiments aiming to determine hemoglobin toxicity to astrocytes cocultured with newborn cortical neurons. Curiously, Figure 7 shows that hemoglobin exerted a toxic effect to astrocytes only when neurons were present in culture. An astrocyte culture with a small neuronal contaminant showed no detectable cytotoxic effect when exposed to hemoglobin (Figure 7C). In contrast, the same hemoglobin concentration

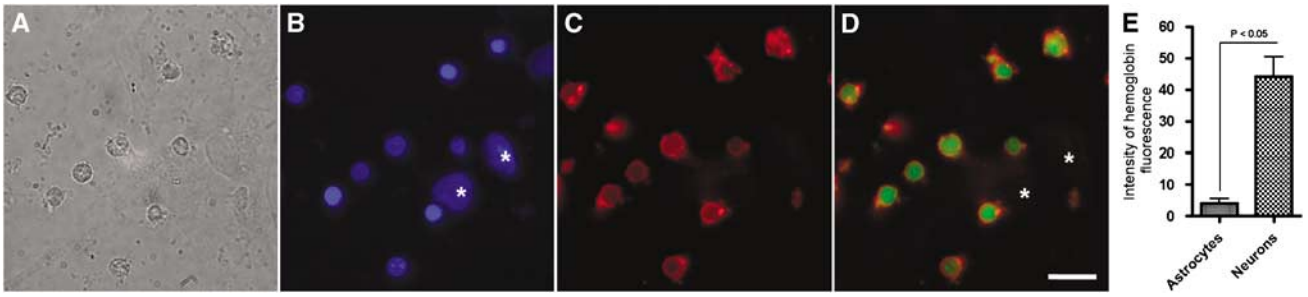

Figure 3 Hippocampal neurons are able to take up hemoglobin *in vitro*. 24 h coculture of astrocytes derived from newborn rat cerebral cortexes and neurons derived from 18-day embryonic rat cerebral hippocampuses were exposed to 0.5 μmol/L hemoglobin conjugated to Alexa 488 for 12 h. (**A**) Phase contrast; (**B**) DAPI fluorescence image showing the presence of two astrocytes (asterisks); (**C**) Anti β-tubulin III immunofluorescence showing the presence of neurons; (**D**) Alexa 488-hemoglobin fluorescence image merged with **C**, showing the absence of hemoglobin uptake by astrocytes compared with stained neurons (asterisks). Scale bar = 10 μm. (**E**) Pixel intensity from hemoglobin median curve fluorescence signal measured by ImageJ software in neurons and astrocytes. Differences of $P < 0.05$ were considered to be significant.

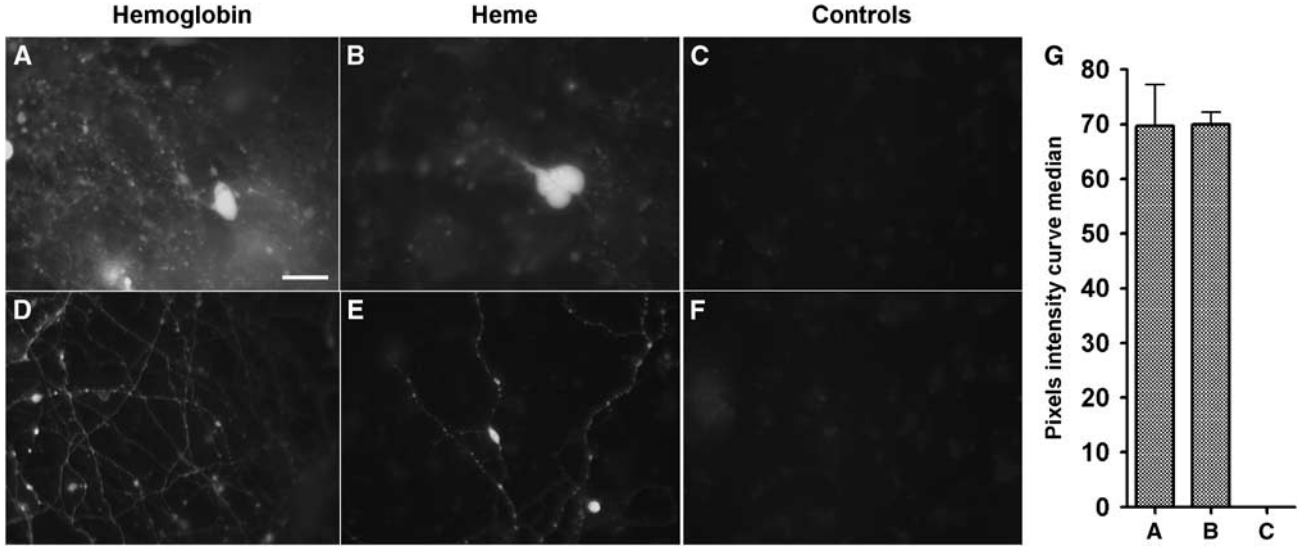

Figure 4 Hemoglobin and heme induce oxidative stress to cortical neurons. Oxidative stress of neurons derived from 18-day embryonic rat cerebral cortexes was evidenced by incubation with 2.5 μmol/L of the reactive probe CMH_2-DCFDA, after exposed to different molecules as follow: (**A** and **D**) 10 μmol/L of hemoglobin; (**B** and **E**) 40 μmol/L of heme; (**C**) 10 μmol/L of albumin; (**F**) 1 μmol/L of staurosporine. (**A**–**C**) High CMH_2-DCFDA fluorescence in cellular bodies; (**D**–**F**) detectable CMH_2-DCFDA fluorescence in neuritis. Scale bar = 10 μm. (**G**) Pixel intensity from CMH_2-DCFDA median curve fluorescence signal measured by ImageJ software in images generated from conditions: A, B, and C.

(10 μmol/L) induced prominent toxic effects to astrocytes when neurons were added to the culture (Figure 7D–7F). Interestingly, a higher cytotoxicity was observed in astrocytes when neuronal density was increased (Figure 7D–7F). To exclude the possibility that intracellular components of senescent neurons would be involved in the astrocytic death related to hemoglobin in cocultures, astrocytes were challenged for 12 h with a conditioned medium of neurons previously exposed to 5 μmol/L staurosporine for 4 h. Viability assays indicated that astrocytes were insensitive to this incubation, suggesting that the effects of hemoglobin on the neuron-derived astrocyte death are not related to any component released by apoptotic neurons (data not shown). Because hemoglobin is not toxic to purified astrocytes (Figure 6), we postulated that neurons exposed to holo-hemoglobin might develop astrocytic toxic properties.

Discussion

Intracerebral hemorrhage is a severe manifestation of cerebral vascular accident, which is highly neurotoxic not only because of the hypoxia generated

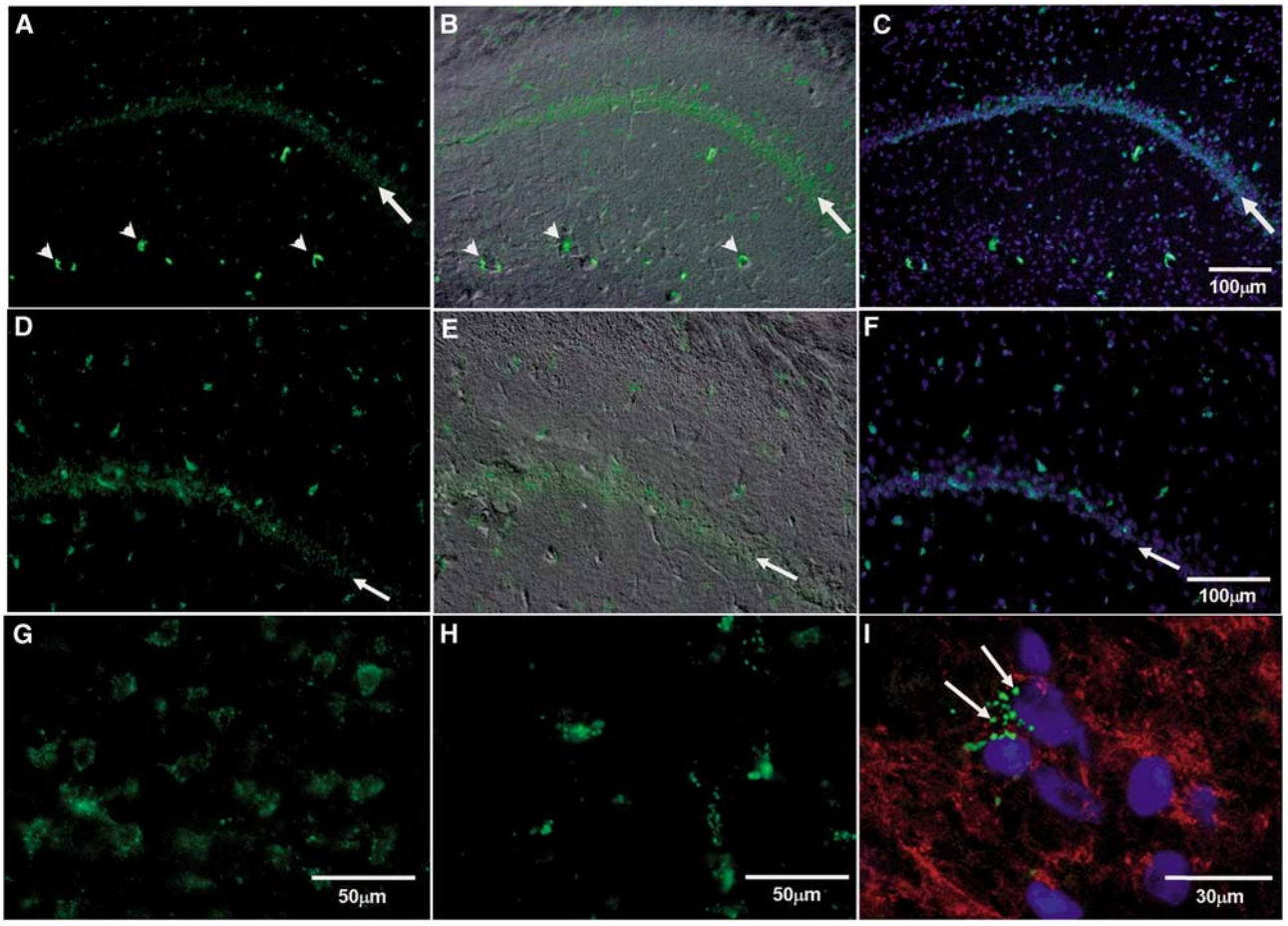

Figure 5 Cortical and hippocampal cells uptake Alexa 488-hemoglobin *in vivo*. Coronal thin sections of brain right hemisphere from adult rats that were stereotaxically injected with 1 μg of hemoglobin-Alexa 488 in the parietal cortex. (**A**, **D**, **G**, and **H**) Alexa 488-hemoglobin signal; (**B** and **E**) interference contrast merged with images **A** and **D**, respectively; (**C** and **F**) DAPI signal merged with images **A** and **D**, respectively; (**I**) confocal β-tubulin III immunolocalization merged with Alexa 488-hemoglobin fluorescence. (**A**–**C**) Alexa 488-hemoglobin punctuated signal in cortex and hippocampus predominantly located in CA1 hippocampal region (arrows) and also strongly associated to blood vessels (arrowhead). (**D**–**F**) Detail of CA1 hippocampal region (arrows) presenting smooth signal distribution, contrasting with punctuated signal presented in cortical and hippocampal cells. (**G** and **H**) Higher magnification of cortical (**G**) or hippocampal (**H**) parenchyma, evidencing hemoglobin-Alexa 488 uptake differences in these two regions of rat brain. (**I**) Parietal cortex presenting β-tubulin III localization stained by CY3, which delineates neurons. Notice the presence of hemoglobin-Alexa 488 green signals inside vesicles (arrows) in some neurons. Nuclei were evidenced by DAPI, in blue. This image is representative of 30 fields from three independent experiments. Scale bar values are indicated in the figure.

by vessel disruption or immunologic response of the parenchyma to blood components, but also because of the deleterious effects of hemoglobin, heme, and iron. Here we show, *in vitro* and *in vivo*, that cortical embryonic neurons are more efficient in taking up hemoglobin as well as the heme analogue SnPPIX than astrocytes (Figures 1, 2, and 3). These results are in agreement with previous data from the literature showing that hemoglobin exerted more powerful toxic effects to neurons than to glial cells (Regan and Panter, 1993). In addition to the clear difference between neuronal and astrocyte hemoglobin and heme uptake, our results open new perspectives on the controversial role of HO-2 in neuronal susceptibility or resistance to heme and hemoglobin (Doré *et al*, 1999; Regan *et al*, 2004). Conceivably, experimental features between different models of *in vitro* ICH would influence neuronal heme and/or hemoglobin uptake, generating the apparent discrepancy of available data.

Heme breakdown by HO generates three products, which severely disturb the function of neural tissue: carbon monoxide, biliverdin, which is immediately converted to bilirubin by biliverdin reductase, and free iron (Ryter and Tyrrell, 2000). The fact that brain HO activity, represented mainly by HO-2, overwhelms that of other organs, including liver and spleen (Zakhary *et al*, 1996), may indicate the major function of their products in cerebral metabolism. Carbon monoxide seems to act as a neuromodulator and, thus, is likely to be involved in cognition,

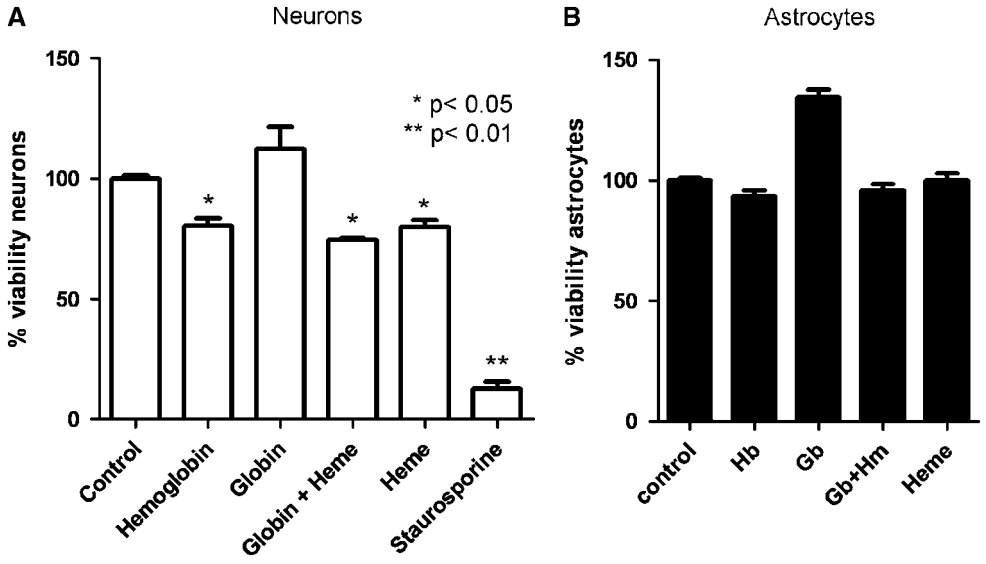

Figure 6 Hemoglobin neurotoxic effects are mediated by heme. Newborn cortical neuron and astrocyte cultures viabilities were measured by observing the reduction of MTT to formazan after exposure for 12 h to different compounds. (**A**) Neurons were exposed to 10 μmol/L globin, 10 μmol/L hemoglobin, 10 μmol/L of hemoglobin reconstituted from globin plus heme, 10 μmol/L heme, or 5 μmol/L staurosporine. Control cultures were performed exposing untreated neurons to MTT. (**B**) Astrocytes were exposed to 10 μmol/L globin, 10 μmol/L hemoglobin, 10 μmol/L of hemoglobin reconstituted from globin plus heme, or 10 μmol/L heme. Control cultures were performed exposing untreated astrocytes to MTT. All experiments were conducted in the presence of polymyxin B (5 μg/mL). Bars represent mean ± s.e.m. Statistical analyses between groups were performed by using analysis of variance and *a posteriori* Tukey's test. Differences of $P < 0.05$ were considered to be significant.

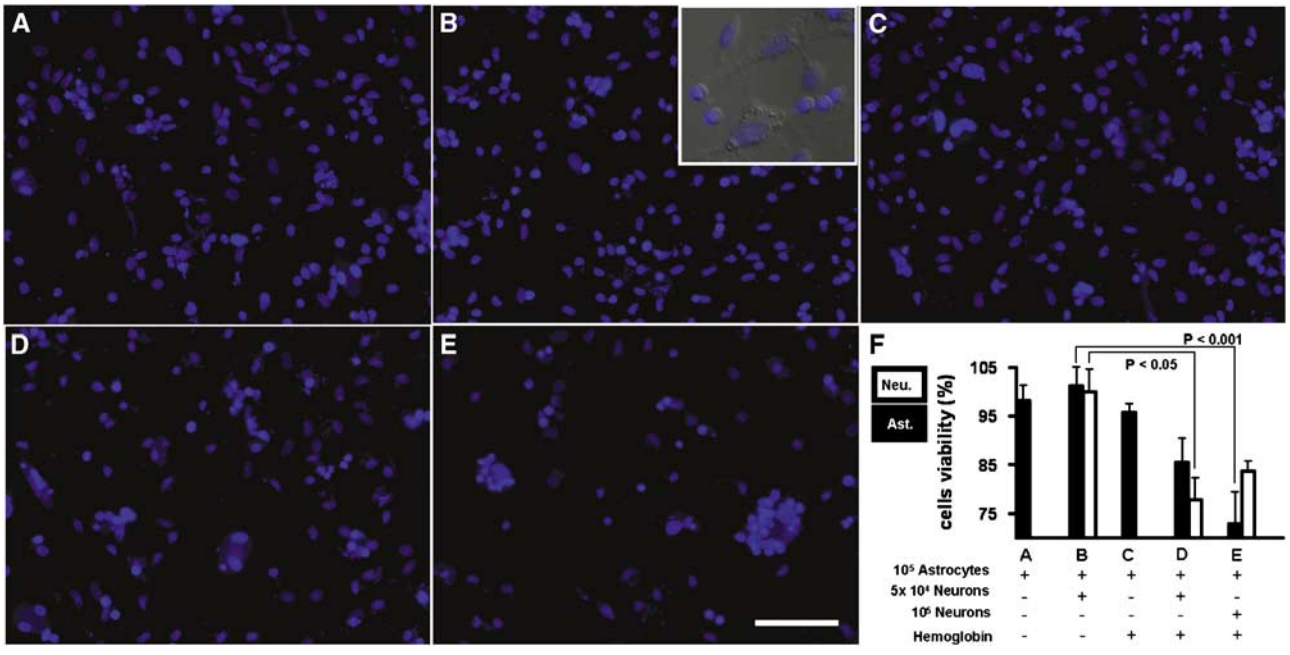

Figure 7 Hemoglobin toxicity is inflicted on astrocytes by neurons. Fluorescence microscopy images of nucleus from neurons and astrocytes cocultures stained by DAPI. (**A**) Astrocytes (10^5) culture control, (**B**) control astrocyte (10^5) and neuron (5×10^4) coculture, (**C**) astrocyte (10^5) exposed to 10 μmol/L hemoglobin for 12 h, (**D**) astrocyte (10^5) and neuron (5×10^4) coculture exposed to 10 μmol/L hemoglobin for 12 h, (**E**) astrocyte (10^5) and neuron (10^5) coculture exposed to 10 μmol/L hemoglobin for 12 h. Scale bar = 50 μm. (**F**) Percentage of viable cells in the conditions described above (letters) estimated by the number of cells per field. Bars represent mean ± s.e.m., white bars represent neurons, and black bars represent astrocytes. Statistical analyses between groups were performed by using analysis of variance and *a posteriori* Tukey's test. Differences of $P < 0.05$ were considered to be significant.

behavioral, and sympathetic activities (Johnson and Johnson, 2000). In addition, carbon monoxide is also able to interact with a number of hemeproteins, including mitochondrial cytochrome *c* oxidase, affecting cellular respiration (d'Amico *et al*, 2006). Interestingly, the distribution of hemoglobin-Alexa 488 uptake in sections of injected brains strongly correlated with blood vessels (Figure 5A and 5B, arrowheads), which is in agreement with findings describing high expression of Toll-like receptor 4 (Zhou *et al*, 2007) and HO-1 (Wang and Doré, 2007) in brain endothelial cells during ICH episodes. Toll-like receptor 4 is a surface receptor involved in innate immune response and its signaling activity has been shown to be activated by heme (Figueiredo *et al*, 2007). Heme detoxification by brain endothelial cells possibly occurs during the initial phase of ICH and could be involved in the protective response against brain edema, based on the vasodilator activity of carbon monoxide in brain microvessels (Zakhary *et al*, 1996). However, some evidence from the literature point out that neurotoxic effects of hemoglobin seems to be dependent of HO-2, as deletion of this isoform not only reduced oxidative stress but also conferred resistance of neurons to hemoglobin (Rogers *et al*, 2003). In addition, HO-2 deletion also protected neurons from heme-induced toxic effects, in a mechanism mediated by oxidative stress (Regan *et al*, 2004). Notwithstanding, astrocyte resistance to hemoglobin is related to HO activity as both pharmacological inhibition by SnPPIX or deletion of *HO-1* gene caused prompt toxic effects associated to both hemoglobin and heme (Regan *et al*, 2000; Chen-Roetling and Regan, 2006). The data presented here shed new light on these aspects because resistance of astrocytes to hemoglobin seems to be related to triggering of a protective response, increasing the expression of HO-1 (Regan *et al*, 2000) but not involving degradation of hemoglobin-derived heme as we clearly show here that astrocytes are much less efficient in the uptake of hemoglobin or heme than neurons (Figures 2C, 3D, and 5). Thus, hemoglobin and heme are able to induce HO-1 expression (Regan *et al*, 2000) by a mechanism that may not involve detectable uptake of these molecules.

Under our experimental conditions, injections of hemoglobin-Alexa 488 into the parietal cortex showed the strongest uptake in the hippocampal region (Figures 5A–5F). Comparisons of hemoglobin uptake between cortical and hippocampal neurons *in vitro* also indicated that neurons from hippocampus were more efficient in hemoglobin uptake (data not shown). Curiously, the regional difference in hemoglobin uptake ability is compatible with differences in HO-2 expression, which is abundant in the hippocampus (Scapagnini *et al*, 2002; Lein *et al*, 2007). Such variations may explain why some regions are more susceptible than others to the damage induced by ICH and could be related to the severity of disabilities observed in patients.

Colocalization of hemoglobin uptake and HO activity led to the conclusion that during intracellular hemoglobin degradation generates free iron, a neurotoxic and pro-oxidant metal. This may explain the mechanisms involved in the benefits of using zinc protoporphyrin IX, a potent HO inhibitor, in ICH events (Gong *et al*, 2006). The negative effects of HO-1 activity in early stages of ICH were already showed by Wang and Doré (2007), observing a reduction in leukocyte infiltration, microglia and macrophage activation, and consequent free radical production in HO-$1^{-/-}$ mice. Thus, controversies on the neuroprotective or neurotoxic effects of HO-2 must take into account the differential uptake of blood products between different brain cells (Doré *et al*, 1999; Rogers *et al*, 2003; Ryter and Tyrrell, 2000).

The data shown in Figure 6A indicate that the well-known neurotoxic effect of hemoglobin (Regan and Panter, 1993; Sadrzadeh *et al*, 1987) is related to the heme moiety but not to the globin polypeptide chain. However, astrocytes showed no sensitivity to any of the blood products tested (globin, hemoglobin, hemoglobin-reconstituted globin, or heme) (Figure 6B). Notwithstanding, a mechanistic explanation for the neurotoxic effect of hemoglobin indicated an involvement of the signaling cascade of protein kinase C and casein kinase 2 activities (Chen-Roetling *et al*, 2008). Further, neurotoxic effects of hemoglobin are mediated by iron regulatory protein 2 that reduces ferritin expression (Chen-Roetling *et al*, 2008).

Death of astrocytes in the perifocal zone and their posterior recolonization has already been described (Koeppen *et al*, 1995). Because astrocytes are extremely resistant to hemoglobin, heme, and hypoxia (Véga *et al*, 2006; Figure 6B), it is likely that the initial gliosis in ICH would be related to the cytotoxic response of neurons during hemoglobin digestion, likewise observed in Figure 7.

In conclusion, we observed that neurons were more efficient in the uptake of globin, hemoglobin, and a heme analogue, compared with astrocytes, resulting in an oxidative stress condition and neurotoxicity. We believe that the involvement of neurons in the immediate response to hemoglobin would be responsible for most of the ICH symptoms. Further work on the mechanisms involved in the preferential uptake of blood products by neurons should lead to potential new tools for ICH treatment.

Acknowledgements

We thank Professor Roberto Lent, from Departamento de Histologia (UFRJ), for the use of stereotactic injection platform; Professor Rosalia Mendez Otero, from Instituto de Biofísica Carlos Chagas Filho (UFRJ), for the use of the cryosection apparatus; Program for Technological Development in Tools for Health—PDTIS-FIOCRUZ; and Dr Bernardo Miguel

Pascarelli, from Departamento de Patologia (FioCruz Foundation), for the use of confocal microscope platform and Professor Ulysses Lins, from Instituto de Microbiologia (UFRJ), for the use of differential interference contrast microscope. We also thank Mrs Rosenilde Holanda for technical assistance; Dr Jorge Marcondes, from Hospital Universitário Clementino Fraga Filho (UFRJ); and Dr João Ricardo Menezes from Departamento de Anatomia (UFRJ), for the scientific discussions. We especially thank Dra Cristina Vidal Pessolani, from Pavilhão Hanseníase (FioCruz Foundation), for all support and comprehension during this project. MFO, AVGS, VMN, and PLO are research scholars from CNPq.

Disclosure/conflict of interest

The authors have no duality of interest to declare.

References

Chen-Roetling J, Regan RF (2006) Effect of heme oxygenase-1 on the vulnerability of astrocytes and neurons to hemoglobin. *Biochem Biophys Res Commun* 350:233–7

Chen-Roetling J, Li Z, Regan RF (2008) Hemoglobin neurotoxicity is attenuated by inhibitors of the protein kinase CK2 independent of heme oxygenase activity. *Curr Neurovasc Res* 5:193–8

d'Amico G, Lam F, Hagen T, Moncada S (2006) Inhibition of cellular respiration by endogenously produced carbon monoxide. *J Cell Sci* 119:2291–8

Doré S, Takahashi M, Ferris CD, Hester LD, Guastella D, Snyder SH (1999) Bilirubin, formed by activation of heme oxygenase-2, protects neurons against oxidative stress injury. *Proc Natl Acad Sci USA* 96:2445–50

Figueiredo RT, Fernandez PL, Mourão-As DS, Porto BN, Dutra FF, Alves LS, Oliveira MF, Oliveira PL, Graça-Souza AV, Bozza MT (2007) Characterization of heme as activator of Toll-like receptor 4. *J Biol Chem* 282:20221–9

Fogelholm R, Nuutila M, Vuorela AL (1992) Primary intracerebral haemorrhage in the Jyvaskyla region, central Finland, 1985–89: incidence, case fatality rate, and functional outcome. *J Neurol Neurosurg Psychiat* 55:546–52

Gomes FC, Garcia-Abreu J, Galou M, Paulin D, Moura Neto V (1999) Neurons induce *GFAP* gene promoter of cultured astrocytes from transgenic mice. *Glia* 26:97–108

Gong C, Hoff JT, Keep RF (2000) Acute inflammatory reaction following experimental intracerebral hemorrhage in rat. *Brain Res* 871:57–65

Gong Y, Tian H, Xi G, Keep RF, Hoff JT, Hua Y (2006) Systemic zinc protoporphyrin administration reduces intracerebral hemorrhage-induced brain injury. *Acta Neurochir Suppl* 96:232–6

Graca-Souza AV, Arruda MA, de Freitas MS, Barja-Fidalgo C, Oliveira PL (2002) Neutrophil activation by heme: implications for inflammatory processes. *Blood* 99:4160–5

Johnson RA, Johnson FK (2000) The effects of carbon monoxide as a neurotransmitter. *Curr Opin Neurol* 13:709–13

Koeppen AH, Dickson AC, McEvoy JA (1995) The cellular reactions to experimental intracerebral hemorrhage. *J Neurol Sci* 134:102–12

Koeppen AH, Dickson AC, Smith J (2004) Heme oxygenase in experimental intracerebral hemorrhage: the benefit of tin-mesoporphyrin. *J Neuropathol Exp Neurol* 63:587–97

Lara FA, Lins U, Bechara GH, Oliveira PL (2005) Tracing heme in a living cell: hemoglobin degradation and heme traffic in digest cells of the cattle tick *Boophilus microplus*. *J Exp Biol* 208:3093–101

Lein ES, Hawrylyc MJ, Ao N *et al* (2007) Genome-wide atlas of gene expression in the adult mouse brain. *Nature* 445:168–76

Lowry OH, Rosebrough NJ, Farr AL, Randall RJ (1951) Protein measurement with the Folin phenol reagent. *J Biol Chem* 193:265–75

Panter SS, Sadrzadeh SM, Hallaway PE, Haines JL, Anderson VE, Eaton JW (1985) Hypohaptoglobinemia associated with familial epilepsy. *J Exp Med* 161:748–54

Porto BN, Alves LS, Fernandez PL, Dutra TP, Figueiredo RT, Graca-Souza AV, Bozza MT (2007) Heme induces neutrophil migration and reactive oxygen species generation through signaling pathways characteristic of chemotactic receptors. *J Biol Chem* 282:24430–6

Regan RF, Chen J, Benvenisti-Zarom L (2004) Heme oxygenase-2 gene deletion attenuates oxidative stress in neurons exposed to extracellular hemin. *BMC Neurosci* 17:5–34

Regan RF, Guo Y, Kumar N (2000) Heme oxygenase-1 induction protects murine cortical astrocytes from hemoglobin toxicity. *Neurosci Lett* 282:1–4

Regan RF, Panter SS (1993) Neurotoxicity of hemoglobin in cortical cell culture. *Neurosc Lett* 153:219–22

Rogers B, Yakopson V, Teng ZP, Guo Y, Regan RF (2003) Heme oxygenase-2 knockout neurons are less vulnerable to hemoglobin toxicity. *Free Rad Biol Med* 35:872–81

Rosen AD, Frumin NV (1979) Focal epileptogenesis after intracortical hemoglobin injection. *Exp Neurol* 66:277–84

Ryter SW, Tyrrell RM (2000) The heme synthesis and degradation pathways: role in oxidant sensitivity. Heme oxygenase has both pro- and antioxidant properties. *Free Rad Biol Med* 28:289–309

Sadrzadeh SM, Eaton JW (1988) Hemoglobin-mediated oxidant damage to the central nervous system requires endogenous ascorbate. *J Clin Invest* 82:1510–5

Sadrzadeh SM, Anderson DK, Panter SS, Hallaway PE, Eaton JW (1987) Hemoglobin potentiates central nervous system damage. *J Clin Invest* 79:662–4

Scapagnini G, D'Agata V, Calabrese V, Pascale A, Colombrita C, Alkon D, Cavallaro S (2002) Gene expression profiles of heme oxygenase isoforms in the rat brain. *Brain Res* 954:51–9

Schmitt TH, Frezzatti WA, Schreierm S (1993) Hemin-induced lipid membrane disorder and increased permeability: a molecular model for the mechanism of cell lysis. *Arch Biochem Biophys* 307:96–103

Simionatto CS, Anderson KE, Sassa S, Drummond GS, Kappas A (1984) Fluorometric measurement of tin-protoporphyrin in biological samples. *Anal Biochem* 141:213–9

Smith MA, Harris PLR, Sayre LM, Perry G (1997) Iron accumulation in Alzheimer disease is a source of redox-generated free radicals. *Proc Natl Acad Sci USA* 94:9866–8

Sudlow CLM, Warlow CP (1997) Comparable studies of the incidence of stroke and its pathological types. Results from an international collaboration. *Stroke* 28:491–9

Teale FW (1959) Cleavage of the haem–protein link by acid methylethylketone. *Biochim Biophys Acta* 35:543

Turner CP, Bergeron M, Matz P, Zegna A, Noble LJ, Panter SS, Sharp FR (1998) Heme oxygenase-1 is induced in glia throughout the brain by subarachnoid hemoglobin. *J Cereb Blood Flow Metab* 18:257–73

Véga CR, Sachleben L, Gozal D, Gozal E (2006) Differential metabolic adaptation to acute and long-term hypoxia in rat primary cortical astrocytes. *J Neurochem* 97:872–83

Wang J, Doré S (2007) Heme oxygenase-1 exacerbates early brain injury after intracerebral haemorrhage. *Brain* 130:1643–52

World Health Organization (2006) *WHO STEPS Stroke Manual: The WHO STEPwise Approach to Stroke Surveillance*. Geneva: World Health Organization

Zakhary R, Gainett SP, Dinerman JL, Ruat M, Flavahant NA, Snyder SH (1996) Heme oxygenase 2: endothelial and neuronal localization and role in endothelium-dependent relaxation. *Proc Natl Acad Sci USA* 93:795–8

Zhou ML, Wu W, Ding YS, Zhang FF, Hang CH, Wang HD, Cheng HL, Yin HX, Shi JX (2007) Expression of Toll-like receptor 4 in the basilar artery after experimental subarachnoid hemorrhage in rabbits: a preliminary study. *Brain Res* 1173:110–6